Simultaneous Reception of Information in the Bidirectional Time Reversal Mirroring System

Charleston Dale M. Ambatali
Electrical and Electronics Engineering Institute
University of the Philippines
Quezon City, Philippines
cmambatali@up.edu.ph

***Abstract*—A resonant beam communication (RBCom) system produces a converging carrier wave between two communicating nodes to maximize power received between them. This is implemented using retroreflective arrays. However, this system only produces a resonant beam on a single frequency point. In the bidirectional time reversal mirroring (BiTRM) system, two communicating nodes use a time reversal mirror device instead, and this produces a similar convergence to the RBCom system but in a wider bandwidth. Analysis of this system in a scattering-rich environment shows that the resulting pulse shape after an infinite number of cycles is the pulse shape that maximizes the energy delivered from one node to the other. As RBCom systems has demonstrated the successful reception of simultaneous signals in the same frequency, the suitability of the BiTRM system to do the same process over a wider bandwidth needs to be investigated. In this paper, we present a simulation experiment to study the performance of BiTRM in receiving two simultaneous signals. Results showed that the lower number of TR cycles at high signal-to-noise ratio values is performs better in terms of bit error rates.**

***Index Terms*—wireless communication, resonant beam, antenna array, retroreflective arrays, time reversal.**

I. Introduction

Time reversal (TR) is a technique that makes use of the reciprocity behavior of a wave to localize the transmitted energy to an intended receiver [1]. It uses multipath components as separate virtual antennas to be able to perform localization [2] as illustrated in figure 1 where an interrogator pulse (ideally an impulse function) is transmitter from the receiver and the recorded signal will be time reversed. The time-reversed signal will be used as a pulse by the transmitter that increases the received signal power at the source of the interrogator.

TR is considered for contactless wireless power transfer [3–5] to increase efficiency. TR also finds its use in improving the performance of communication systems in severe multipath conditions [6, 7]. As it is a form of matched filtering, TR increases the signal-to-noise ratio (SNR) at the receiver.

Despite its ability to increase the signal power at the receiver, TR is not the optimum waveform for the maximum power delivered. If the goal is maximum received power or energy, then the pulse derived from the power waveforming (PW) technique is the optimal solution [8]. It requires complete information about the channel impulse response (CIR) from which a discrete-time waveform is derived. However, in a practical setting, information about the channel is estimated. Doing so will increase the time needed by the transmitter to compute the waveform.

Although the formulation for both techniques stems from different needs, by letting two communicating devices perform

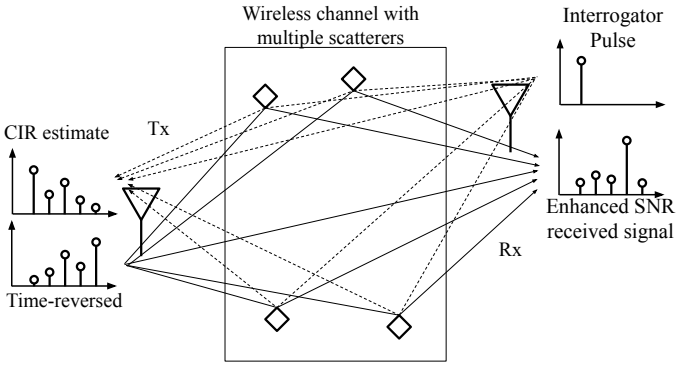

Fig. 1. Illustration of the time reversal concept.

TR back and forth, it can be shown that the PW pulse is generated after an infinite amount of time. Even if a long time is needed, a finite number of cycles can generate a good estimate of the optimal TW pulse, thus reducing the time and overhead needed to perform the technique and eliminating the need for channel estimation.

In this paper, we characterize the behavior of this bidirectional TR mirroring (BiTRM) implementation. We also investigate its ability to receive simultaneous signals from two sources with one receiver. Through a simulation, we compared its bit error rate (BER) performance under a noisy severe multipath environment with the classical TR technique, the PW technique, and the rectangular pulse. It is also in simulation that the performance of BiTRM is evaluated with its ability to separate the information from two users simultaneously being received.

II. Math Notation

We denote lowercase bold font characters ($\mathbf{h}$) as vectors, uppercase bold font ($\mathbf{H}$) characters as matrices, and italicized characters (h) as scalar values. $\mathbf{H}^T$ to be the transpose of $\mathbf{H}$, and $\mathbf{H}^*$ is the conjugate transpose of $\mathbf{H}$. The conjugate of scalar value h is denoted by $\bar{h}$ and the per-element conjugation of a vector $\mathbf{h}$ and matrix $\mathbf{H}$ are written as $\bar{\mathbf{h}}$ and $\bar{\mathbf{H}}$, respectively.

In the subsequent analyses for BiTRM, we represent a discrete-time signal by a vector with a certain length corresponding to the value of the signal at different time indices. For a pulse $\mathbf{h} \in \mathbb{C}^{L\times 1}$, We define $\mathbf{h}^\dagger = \begin{bmatrix}\bar{h}_{L-1} & \bar{h}_{L-2} & \dots & \bar{h}_1 & \bar{h}_0\end{bmatrix}^T$ as the time-reversed pulse of $\mathbf{h}$. Convolution is represented by a matrix multiplication defining $\mathbf{H} \in \mathbb{C}^{L\times L}$ as a Toeplitz matrix expressed as in equation (1) of some CIR represented by $\mathbf{h}$.

979-8-3315-6946-4/25/$31.00 ©2025 IEEE

$$\mathbf{H} = \begin{bmatrix} h_0 & 0 & 0 & ... & 0 & 0 \\ h_1 & h_0 & 0 & ... & 0 & 0 \\ \vdots & \vdots & \ddots & \ddots & \vdots & \vdots \\ h_{L-1} & h_{L-2} & ... & ... & h_0 & 0 \\ 0 & h_{L-1} & ... & ... & h_1 & h_0 \end{bmatrix} \tag{1}$$

By consequence, the time-reversed output of the convolution operation $\mathbf{y} = \mathbf{H}\mathbf{x}$ for some output $\mathbf{y} \in \mathbb{C}^{L\times 1}$ and input $\mathbf{x} \in \mathbb{C}^{L\times 1}$, can be expressed as $\mathbf{y}^\dagger = \mathbf{H}^*\mathbf{x}^\dagger$.

III. Resonant Beam Communication

A. RBCom system architecture

The block diagram of the resonant beam system is shown in figure 2. From the receiver side, an unfocused pilot signal is sent from the receiver through the channel. It can be represented by a vector $\mathbf{a}_2$ whose elements corresponds to an input to a respective individual antenna element. This is received by the transmitter antenna array as $\mathbf{S}^T\mathbf{a}_2$, and is conjugated as per retrodirective operation [11]. The output of the generator, $\mathbf{a}_1$, comes back to the receiver through the same channel which is received as $\mathbf{S}\mathbf{a}_1$.

$\mathbf{S}$ represents a flat fading multiple input multiple output channel. Its elements correspond to the fading experienced by the signal from one transmit element to one receiving element. Due to the reciprocity property of electromagnetic waves, the channel experienced from receiver to transmitter is represented by the transpose of $\mathbf{S}$. A more detailed derivation of the behavior of this system is done in a previous work by the author [10] in its application to wireless power transfer.

B. Analysis of behavior

The discrete-time characteristic equation of figure 2 can be expressed as equation (2), where one sampling period is assumed to be the sum of the round-trip time of the signal from the receiver side to the generator side and the processing delay of the other system components.

$$\mathbf{a}_1^{(k)} = \mathbf{S}^H\mathbf{S}\mathbf{a}_1^{(k-1)} \tag{2}$$

The response of the system for an arbitrary initial condition is given by equation (3). Here, $\mathbf{v}_i$ is an eigenvector of $\mathbf{S}^H\mathbf{S}$ and a_{1i} are weights for $\mathbf{a}_1$.

$$\mathbf{a}_1^{(k)} = \sum_i \xi_i^k a_{1i}^{(0)}\mathbf{v}_i, \tag{3}$$

The resulting steady state expressions in marginal stability are given by equation (4). Working with the assumption that $\mathbf{a}_1$ is always set to maintain some constant power, then equation (4) is the resulting expression after a long time passes.

$$\lim_{k\to+\infty} \mathbf{a}_1^{(k)} = (\xi_{max})^k a_{1,max}^{(0)}\mathbf{v}_{max}. \tag{4}$$

Since steady state value of $\mathbf{a}_1$ is a scalar multiple of $\mathbf{v}_{max}$, then the power transferred frrom transmitter to receiver is maximized.

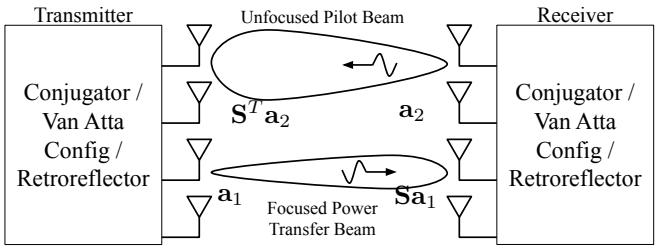

Fig. 2. Diagram of the resonant beam architecture [9, 10].

IV. Bidirectional Time Reversal Mirror

A. Brief overview of waveforming

Waveforming is the synthesis of pulse shapes in wireless communications to overcome wideband small-scale signal propagation losses [2]. It uses scatterers in the channel as virtual antennas to focus power at the intended receiver at a specific time index as the pulse aligns with the CIR. In the context of a stochastic channel like the wireless channel, the time reversal (TR) [6] and power waveforming (PW) [8] techniques are two methods that stand out. The former attempts to achieve the matched filter condition while the latter calculates the pulse that maximizes power at the intended receiver.

In the TR technique, to generate the pulse shape, the receiver must send an impulse that will be sampled and recorded by the transmitter. This recorded signal will be time reversed and conjugated. If $\mathbf{s}_{tr}$ is the pulse shape, then mathematically, it is expressed as in equation (5) where $\left(\sqrt{\mathbf{h}^*\mathbf{h}}\right)^{-1}$ is a scalar factor that normalizes the energy of the pulse to unity. If $\mathbf{x} = \mathbf{s}_{tr}$, then the output $\mathbf{y}$ will have a maximum value equal to $\left(\sqrt{\mathbf{h}^*\mathbf{h}}\right)^{-1}$.

$$\mathbf{s}_{tr} = \begin{bmatrix} \bar{h}_{L-1} & \bar{h}_{L-2} & ... & \bar{h}_0 \end{bmatrix}^T \left(\sqrt{\mathbf{h}^*\mathbf{h}}\right)^{-1} \tag{5}$$

In the PW technique, the goal is for the energy E, to be maximized at the receiver. Mathematically, $E = \mathbf{y}^*\mathbf{y}$ and using $\mathbf{y} = \mathbf{H}\mathbf{x}$, it can be expressed as $E = \mathbf{x}^*\left(\mathbf{H}^*\mathbf{H}\right)\mathbf{x}$. The PW pulse denoted by $\mathbf{s}_{pw}$ requires solving for $\mathbf{x}$ that maximizes E constrained by the condition that $\mathbf{s}_{tr}^*\mathbf{s}_{tr} = 1$. This can be expressed by the formulation in equation (6).

$$\mathbf{s}_{pw} = \arg\max_{\mathbf{x}} \left\{ \frac{\mathbf{x}^*\left(\mathbf{H}^*\mathbf{H}\right)\mathbf{x}}{\mathbf{x}^*\mathbf{x}} \right\} \tag{6}$$

The solution to the above problem is the eigenvector of $\mathbf{H}^*\mathbf{H}$ that is associated with its maximum eigenvalue. Moreover, since $\mathbf{H}^*\mathbf{H}$ is a Hermitian matrix, all its eigenvalues are real numbers. If $\mathbf{x} = \mathbf{s}_{pw}$, an additional matched filtering is needed at the receiver to obtain the benefits of the TR waveform. The maximum value of the output of this is equal to the square root of the maximum eigenvalue of $\mathbf{H}^*\mathbf{H}$.

B. BiTRM system architecture

As waveforming or pulse-shaping is the time domain analogue to beamforming in the spatial domain, then TR is the time domain analogue to a retrodirective antenna array in the spatial domain. That is, both devices can focus their generated beam towards the source of the pilot/interrogator signal. By placing a retrodirective antenna array on the transmitter and the receiver, a resonant beam system is formed [9, 12] as characterized in the preceding section.

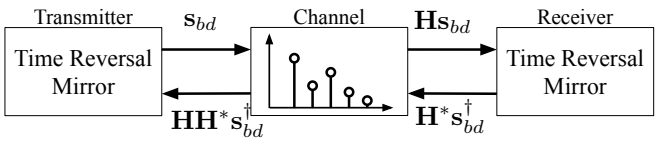

Fig. 3. Diagram of the bidirectional time reversal mirroring (BiTRM) system.

Since the retrodirective array uses phase conjugation at a single frequency point, a connection can be made with the TR technique as time reversal in the time domain corresponds to wideband conjugation in the frequency domain. Therefore, by using a TR mirror on both transmitter and the receiver sides, we hypothesize that a pulse that maximizes power transfer must be generated similar to the operation of the resonant beam system. The block diagram of this setup is shown in figure 3.

C. Analysis of behavior

To analyze the behavior of the proposed BiTRM, the analysis of the resonant beam system can be used as a reference [13]. From figure 3, we denote $\mathbf{s}_{bd}^{(k)}$ as the pulse shape generated by the transmitter at the k^{th} time index. At the receiver side, the received signal can be written as $\mathbf{Hs}_{bd}^{(k)}$, and subsequently time-reversed. The result becomes $\mathbf{H}^*\mathbf{s}_{bd}^{\dagger(k)}$ and this also passes through the channel. The transmitter receives a new signal, $\mathbf{HH}^*\mathbf{s}_{bd}^{\dagger(k)}$ that is time-reversed again. Then, a new pulse shape $\mathbf{s}_{bd}^{(k+1)}$ is generated and the process repeats itself.

The above explanation can be captured by the formulation shown in equation (7). Let $\mathbf{H}^*\mathbf{H}$ have a set of eigenvalues denoted by $\{\lambda_i\}$ corresponding to eigenvectors $\{\mathbf{h}_{e,i}\}$. Any discrete-time signal $\mathbf{x}$ can be expressed as a sum of $x_i\mathbf{h}_{e,i}$ for all i where x_i is the component of $\mathbf{x}$ mapped onto the eigenvector $\mathbf{h}_{e,i}$.

$$\mathbf{s}_{bd}^{(k+1)} = \mathbf{H}^*\mathbf{H}\mathbf{s}_{bd}^{(k)} \tag{7}$$

Given an initial condition $\mathbf{s}_{bd}^{(0)}$ with the initial vector components denoted by $s_i^{(0)}$, the general form of $\mathbf{s}_{bd}^{(k)}$ can be expressed as in equation (8). If for each cycle of TR mirroring, the resulting pulse is normalized to unity energy, i.e., $\mathbf{s}_{bd}^{(k)*}\mathbf{s}_{bd}^{(k)} = 1$, then the maximum eigenvalue λ_{max} is unity. Therefore, if $k \to +\infty$, since $\lambda_i < 1$ for all $i \neq max$, then the final expression becomes equation (9).

$$\mathbf{s}_{bd}^{(k)} = \sum_i \lambda_i^k s_i^{(0)}\mathbf{h}_{e,i} \tag{8}$$

$$\lim_{k\to+\infty} \mathbf{s}_{bd}^{(k)} = \lambda_{max}^k s_{max}^{(0)}\mathbf{h}_{e,max} \tag{9}$$

D. Suitability for simultaneous reception of signals

Consider two users simultaneously sending data to a single receiver (base station). The block diagram illustrating this can be seen in figure 4. Each user experiences the same severity of multipath fading but uncorrelated. Let $\mathbf{H}_1$ and $\mathbf{H}_2$ be the Toeplitz matrix of their respective CIRs, $\mathbf{s}_1$ and $\mathbf{s}_2$ be their respective pulse shapes, and x_1 and x_2 be the transmitted symbols. By transmitting simultaneously, the received signal vector $\mathbf{y}$ can be expressed as in equation (10).

$$\mathbf{y} = \mathbf{H}_1\mathbf{s}_1x_1 + \mathbf{H}_2\mathbf{s}_2x_2 \tag{10}$$

The matched pulse filters at the receiver aims to separate the two signals from each other. By sampling at the time indices that maximizes the value of the signal, the resulting estimated symbols can be written as equation (11).

$$\begin{aligned}\hat{x}_1 &= \mathbf{s}_1^H\mathbf{H}_1\mathbf{s}_1 + \mathbf{s}_1^H\mathbf{H}_2\mathbf{s}_2 \\ \hat{x}_1 &= \mathbf{s}_2^H\mathbf{H}_1\mathbf{s}_1 + \mathbf{s}_2^H\mathbf{H}_2\mathbf{s}_2\end{aligned} \tag{11}$$

If the pulses used are the PW pulses, i.e. $\mathbf{s}_1 = \mathbf{s}_{bd1}$ and $\mathbf{s}_2 = \mathbf{s}_{bd2}$, then the expected values of $\mathbf{s}_1^H\mathbf{H}_2\mathbf{s}_2$ and $\mathbf{s}_2^H\mathbf{H}_1\mathbf{s}_1$ are zero as long as the timing of the arrivals of the signals, as defined by $\mathbf{H}_1$ and $\mathbf{H}_2$ do not coincide.

V. Simulation

A. Over-all block diagram and flow

The block diagram of the simulation system is shown in figure figure 4. First, the system generates two random stream of bits which are mapped onto a quadrature phase shift keying (QPSK) constellation. The QPSK symbols will be upsampled by D samples per symbol and subsequently be shaped through pulse shaping filter with L coefficients defined by the respective pulse shape $\mathbf{s}$ of the different techniques compared. The resulting

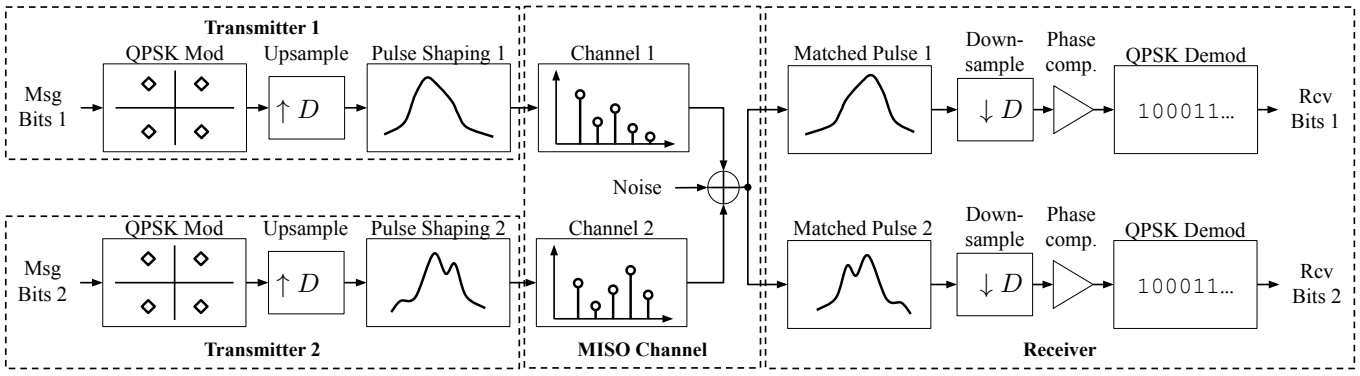

Fig. 4. Block diagram of the simulation setup. On each transmitter, uncorrelated streams of random bits generated are mapped to QPSK symbols, then upsampled. The pulse shaping filters will use the pulses from the TR technique, PW technique, and BiTRM derived from the respective CIR they experience. At the receiver, noise is added before two matched filters that is intended to separate the two transmitters. Their outputs are downsampled at time indices that maximize SNR, phase compendated, and then converted back to bits.

signal passes through different uncorrelated Rayleigh fading channels with impulse responses $\mathbf{h}_{c1}$ and $\mathbf{h}_{c2}$, both having a length L. White Gaussian noise is added at the receiver. An estimate of the QPSK symbols is recovered after using respective matched filters whose coefficients are the time reversal of the pulse shapes used per transmitter. Downsampling by a factor of D is performed at time indices that maximize the SNR for each pulse shape. Phase and amplitude correction is performed for each stream to get an estimate of the QPSK symbol sent in that stream. Finally, they are converted to bits from which the number of errors are determined.

The simulator loops the above process until it reaches a minimum number of bit errors (set to 10 bits) or if the maximum number of bits (set to 10^9 bits) has been exceeded. Each simulation is performed at different levels of noise power.

The parameter L (CIR length) is also varied to test the robustness of the techniques at different pulse lengths. In this simulatin, we let $D = L$ simulating a narrowband wireless channel. The difference in the time of arrival of the two Rayleigh channels are also varied.

B. Channel model

The CIR is denoted by the column vectors $\mathbf{h}_{c1}, \mathbf{h}_{c2} \in \mathbb{C}^{L\times 1}$. Each element is a representation of a single path from the respective transmitter to the receiver sampled at different times. All of the elements are complex Gaussian random variables with variance dependent on the average power of the respective path.

The parameter L denotes the severity of the multipath effect of the channel. Larger values correspond to a longer delay spread. For the succeeding results discussed, the simulation used a mean path gain profile expressed in equation (12) for both channels where $k \in \{0, ..., L-1\}$ and α is a parameter that defines how fast the power degrades.

$$\mathbb{E}\left\{|\mathbf{h}_c[k]|^2\right\} = 10^{-\alpha k} \tag{12}$$

Another parameter that is varied is the difference between the time of arrival of the two users transmitting to a single receiver. Its effect is apparent when separating the two signals at the matched filters. For the case when $x_1 = x_2 = 1$ and a given CIR, the output at the matched filters before the downsampling blocks when using the respective PW pulses is shown in figure 5.

C. Waveforming methods compared

The TR pulse, PW pulse, and the BiTRM pulse shapes are compared. The TR pulse is generated by getting the time-reversed conjugate of $\mathbf{h}_c$ normalized to unity while the PW pulse is computed from the Toeplitz version of $\mathbf{h}_c$ assuming complete information is known.

Two cases of pulses produced through BiTRM are tested. One case uses 5 cycles while the other uses only 2 cycles. The initial condition to generate these pulses start from an impulse signal. While the simulator computes the convolution of the channel impulse response, only the first L samples are committed to memory while the rest of the convolution result is discarded. Finally, a rectangular pulse of length L is used as a control setup.

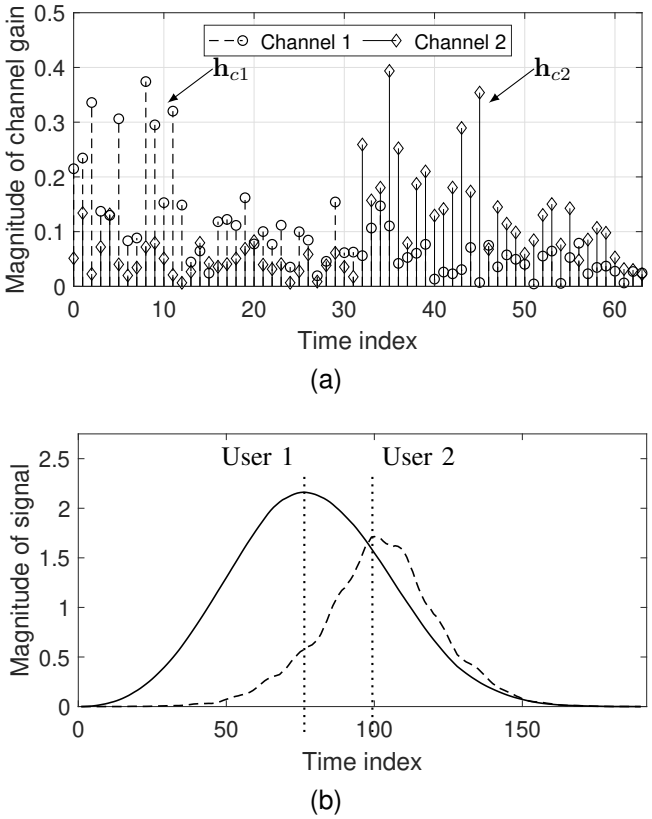

Fig. 5. A visualization of the difference in arrival time as defined by the (a) channel impulse response resulting into (b) the respective outputs after the matched filter blocks from figure 4.

VI. Results and Discussion

A. Single user case

Figure 6 shows the performance of the different pulse shapes under different SNR values. It can be observed that the PW pulse outperforms all other pulse shapes followed by the BiTRM pulses in which the 5-cycle pulse performs better than the 2-cycle pulse. This is due to the higher SNR achieved by the PW technique as it is the pulse that enables maximum energy to be delivered to the intended receiver. Since BiTRM approximates the PW pulse shape as more TR cycles pass, its performance approaches that of the PW pulse.

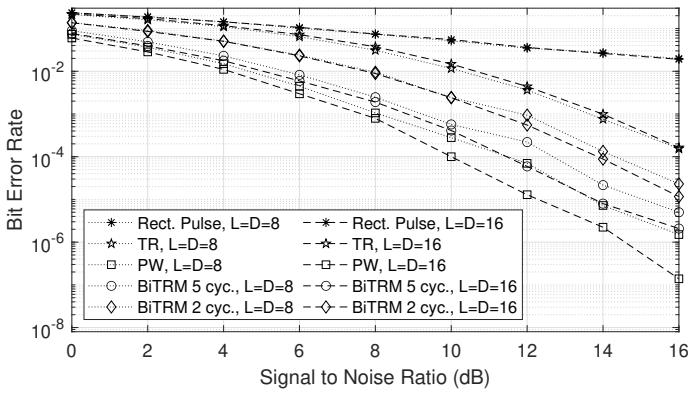

Fig. 6. BER performance of the different pulse shapes vs. SNR CIR length of 24 and 32 time indices.

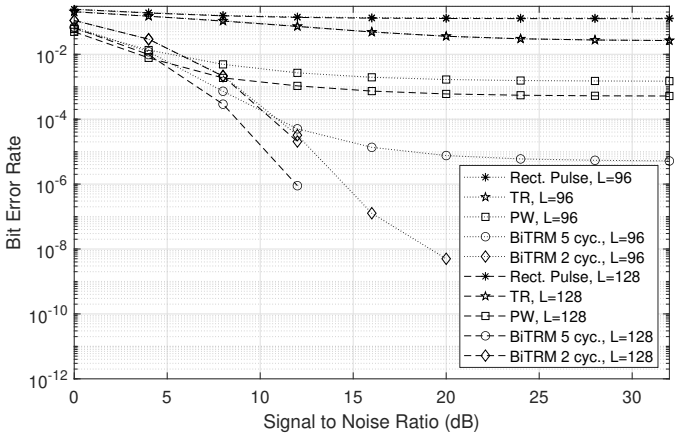

(a)

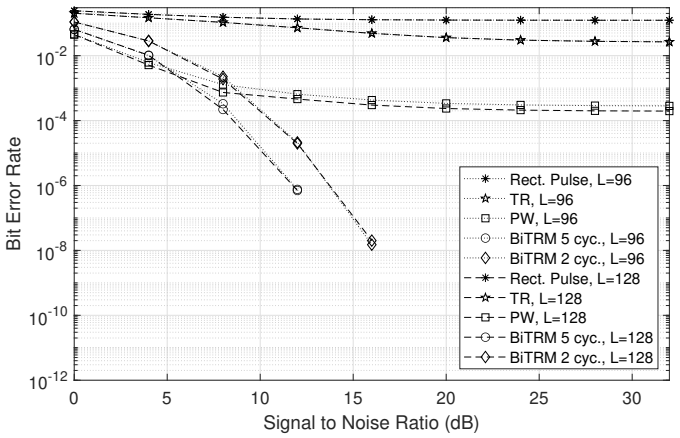

(b)

Fig. 7. BER performance of the different pulse shapes vs SNR when two users simultaneously transmit to one receiver on the same frequency bands experiencing uncorrelated fading. (a) CIR length of 32 and 64 and (b) CIR length of 96 and 128.

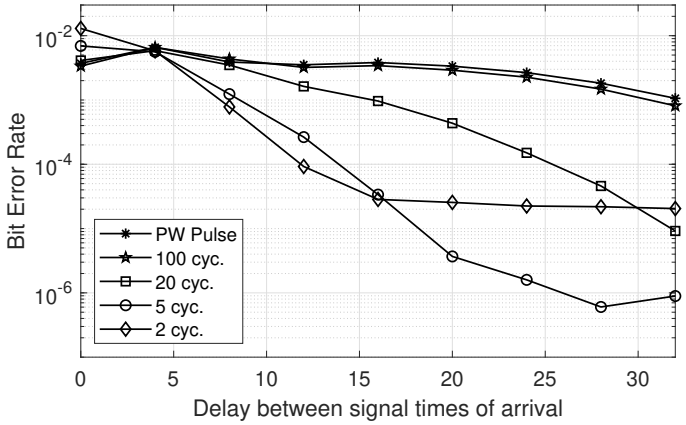

(a)

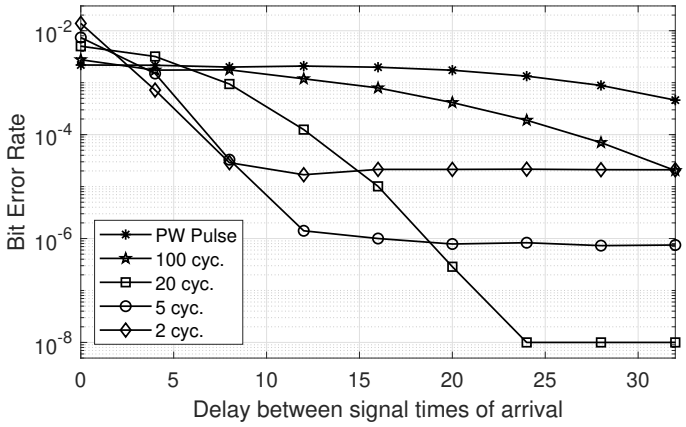

(b)

Fig. 8. BER performance when two users simultaneously transmit vs. varying difference between the times of arrival of the signals at 12 dB SNR: (a) CIR length of 64 and (b) CIR length of 128.

B. Two simultaneous users

For the two simultaneous users case, figure 7 shows the results for different CIR lengths assuming that the difference in times of arrival between the users are half the CIR length. Figure 7a shows the case when $L = 32$ and $L = 64$, while figure 7b shows $L = 96$ and $L = 128$. Generally, the the BiTRM and PW pulses outperform the TR and rectangular pulses in terms of BER.

At low SNR values, the PW pulse performs best, but it hits a minimum BER floor as SNR increases. On the other hand, the BiTRM pulses are observed to have a BER floor that is less than that of the PW pulse. Moreover, having more cycles for BiTRM decreases the BER as is the case for a single user transmission. However, the pulse produced by BiTRM as $k \to +\infty$ is the PW pulse. Therefore, it is expected that an optimum number of cycles will improve the performance to an optimum low BER before it increases again to that of the PW pulse.

To observe the effect of the varying the difference between arrival times of the users, the performance of the PW pulse and BiTRM pulse with varying number of cycles is evaluated at 12 dB SNR and with $L = 64$ and $L = 128$. The result of this is shown in figure 8. It is observed that the BiTRM with 5 cycles perform the best as the difference in times of arrival of the users are larger for $L = 64$ and 20 cycles for $L = 128$. However, a downward trend on the BER of the higher number of cycles suggest that as the PW pulse is approximated and if the difference in times of arrival is larger, then a better performance can be expected. Over-all, this test shows how BiTRM is suitable for simultaneous reception of two signals operating in the same frequency, in a multipath-rich environment, at a high SNR level.

VII. Conclusion

In this paper, we introduced and analyzed the bidirectional time reversal mirroring system (BiTRM) as an extension and combination of the time reversal technique and the resonant beam system. We further characterized its behavior which is shown to be in parallel of the resonant beam system in which the pulse design created by BiTRM approaches the power waveforming (PW) pulse predicted in theory analogous to the resonant beam system approaches the configuration for maximum energy delivered to the intended receiver.

Through a simulation, we demonstrated the superiority of the proposed BiTRM system over other pulse designs, namely the TR pulse and the PW pulse. While the PW pulse outperforms

BiTRM in the single user case, the BiTRM pulse design is better suited to accommodate two simultaneous signals operating in the same frequency band with reasonable BER performance at high SNR values as long as the users' signals arrive at the receiver at different times.

Recommendation for further work on this is to characterize the multi-user performance of BiTRM and find a theoretical maximum number of users it can support simultaneously. Further analysis on its performance with varying CIR length, difference between arrival times, and SNR is also recommended in the multi-user case.

ACKNOWLEDGMENT

The author acknowledges the Office of the Chancellor of the University of the Philippines Diliman, through the Office of the Vice Chancellor for Research and Development, for funding support through the PhD Incentive Award Grant 252510 YEAR 1.

REFERENCES

[1] P. H. Siegel, "IEEE President K. J. Ray Liu, "Follow Multiple Paths," Changing the World With Microwave Time Reversal Focusing," *IEEE Journal of Microwaves*, vol. 2, no. 3, pp. 360–373, Jul. 2022, ISSN: 2692-8388.

[2] Q. Xu, C. Jiang, Y. Han, B. Wang, and K. J. R. Liu, "Waveforming: An Overview With Beamforming," *IEEE Communications Surveys & Tutorials*, vol. 20, no. 1, pp. 132–149, 2018, ISSN: 1553-877X.

[3] Z. Wang, J. Hu, K. Yang, and K.-K. Wong, "Wideband Waveforming for Integrated Data and Energy Transfer: Creating Extra Gain Beyond Multiple Antennas and Multiple Carriers," *IEEE Transactions on Wireless Communications*, vol. 23, no. 4, pp. 2855–2868, Apr. 2024, ISSN: 1558-2248.

[4] H. S. Park and S. K. Hong, "Investigation of Time-Reversal Based Far-Field Wireless Power Transfer From Antenna Array in a Complex Environment," *IEEE Access*, vol. 8, pp. 66 517–66 528, 2020.

[5] P. Lu, M. Wagih, G. Goussetis, N. Shinohara, and C. Song, "A Comprehensive Survey on Transmitting Antenna Systems With Synthesized Beams for Microwave Wireless Power Transmission," *IEEE Journal of Microwaves*, vol. 3, no. 4, pp. 1081–1101, 2023.

[6] J. Wang and J. Lian, "Time-reversal waveform design for underwater wireless optical communication systems," EN, *Optics Express*, vol. 31, no. 19, pp. 31 447–31 462, Sep. 2023, Publisher: Optica Publishing Group, ISSN: 1094-4087.

[7] Y. Kida, M. Deguchi, K. Okadome, Y. Watanabe, and T. Shimura, "Experimental demonstration of high spectral efficiency MIMO underwater acoustic communication using adaptive passive time reversal on the continental shelf in mid latitude," in *OCEANS 2023 - Limerick*, 2023, pp. 1–6.

[8] M.-L. Ku, Y. Han, H.-Q. Lai, Y. Chen, and K. J. R. Liu, "Power Waveforming: Wireless Power Transfer Beyond Time Reversal," *IEEE Transactions on Signal Processing*, vol. 64, no. 22, pp. 5819–5834, Nov. 2016, ISSN: 1941-0476.

[9] Y. Tian, D. Li, C. Huang, Q. Liu, and S. Zhou, "Resonant Beam Communications: A New Design Paradigm and Challenges," *Journal of Communications and Information Networks*, vol. 9, no. 1, pp. 80–87, Mar. 2024, ISSN: 2509-3312.

[10] C. D. Ambatali, S. Nakasuka, B. Yang, and N. Shinohara, "Analysis and experimental validation of the WPT efficiency of the both-sides retrodirective system," *Space Solar Power and Wireless Transmission*, vol. 1, no. 1, pp. 48–60, 2024, ISSN: 2950-1040.

[11] R. Miyamoto and T. Itoh, "Retrodirective arrays for wireless communications," *IEEE Microwave Magazine*, vol. 3, no. 1, pp. 71–79, 2002.

[12] T. Matsumuro, Y. Ishikawa, and N. Shinohara, "Basic study of both-sides retrodirective system for minimizing the leak energy in microwave power transmission," *IEICE Transactions on Electronics*, vol. 102, no. 10, pp. 659–665, 2019.

[13] C. D. M. Ambatali and S. Nakasuka, "Characterizing the Dynamic Behavior of a Both-Sides Retrodirective System for the Control of Microwave Wireless Power Transfer," in *2024 SICE International Symposium on Control Systems (SICE ISCS)*, 2024, pp. 99–106.